RSC Advances

PAPER

View Article Online
View Journal | View Issue

Check for updates

Cite this: *RSC Adv.*, 2024, **14**, 13129

The conjugates of 5′-deoxy-5-fluorocytidine and hydroxycinnamic acids – synthesis, anti-pancreatic cancer activity and molecular docking studies†

Marcin Cybulski, *[a] Magdalena Zaremba-Czogalla, [b] Bartosz Trzaskowski, [c] Marek Kubiszewski, [d] Joanna Tobiasz,[a] Anna Jaromin, [b] Piotr Krzeczyński, [a] Jerzy Gubernator [b] and Olga Michalak *[a]

Received 4th March 2024
Accepted 15th April 2024

DOI: 10.1039/d4ra01683a

rsc.li/rsc-advances

New amide conjugates **1–6** of hydroxycinnamic acids (HCA) and 5′-deoxy-5-fluorocytidine (5-dFCR), the prodrug of 5-fluorouracil (5-FU), were synthesized and tested *in vitro* against pancreatic cancer lines (PDAC). The compounds showed slightly higher efficacy against primary BxPC-3 cells (IC_{50} values of 14–45 μM) than against metastatic AsPC-1 (IC_{50} values of 37–133 μM), and similar to that of 5-FU for both PDAC lines. Compound **1**, which has a *para*-(acetyloxy)coumaroyl substituent, was found to be the most potent (IC_{50} = 14 μM) with a selectivity index of approximately 7 to normal dermal fibroblasts (IC_{50} = 96 μM). The potential pharmacological profiles were discussed on the basis of the ADME data. Docking to the carboxylesterase CES2 showed that the synthesized compounds have the ability to bind *via* hydrogen bonding between a specific acetate group of the sugar moiety and Ser228, which belongs to the catalytic triad that causes hydrolysis. Docking to albumin, a major transport protein in the circulatory system, revealed a strong interaction of the conjugates at the binding site which is native to warfarin and responsible for its transport in the body.

Open Access Article. Published on 23 April 2024. Downloaded on 12/9/2025 12:17:06 AM.
This article is licensed under a Creative Commons Attribution-NonCommercial 3.0 Unported Licence.

Introduction

Combination therapy with drugs targeting a different or similar pathway is the gold standard in oncological treatments.[1–5] In addition to the efficient therapies with anticancer cocktails,[6] the effective combination therapy of natural plant medicines and known anticancer drugs has been reported in a limited number of studies. Lee *et al.*[7] postulated the benefits in postoperative gastric cancer patients in terms of overall and disease-free survival after chemotherapy supported by traditional herbal medicines. Kamran *et al.*[8] evidenced a synergistic effect in HCT116 colon cancer cells after co-administration of 5-fluorouracil and diosmetin. However, for some types of cancer, there are still limitations that need to be overcome to achieve a better survival rate. Besides, in some clinical analyses, the combination therapies afford predictable and clinically unsignificant benefits.[9] The obstacles of multidrug therapies require work on more effective anti-cancer drugs. One of the directions is to design and study single molecules that combine structures of more than one anti-cancer drug or contain their haptophore fragments.[10–12] The other approach is based on the conjugation of a known anticancer agent with a molecule that allows targeted delivery to tumour cells. As a result of research, eleven antibody-drug conjugates for cancer therapy have already been approved by FDA.[13,14] Furthermore, glufosfamide, the first sugar conjugate of DOX, is still under investigation to determine whether it provides additional survival benefit in patients with metastatic pancreatic cancer after gemcitabine-based first-line regimen.[15]

Since the 1960s, 5-fluorouracil (5-FU) has been used as a time-dependent antimetabolite in the treatment of diverse types of malignancies.[16] The effectiveness of oral 5-FU is limited due to its low bioavailability related to poor membrane permeability and GIT absorption.[17] Therefore, continuous intravenous infusion of 5-FU is the most effective chemotherapeutic regimen.[18] In the last four decades of the 20th century, various clinical trials showed that oral 5-FU prodrugs could be similarly effective to continuous infusion of 5-FU. Two orally administered prodrugs, tegafur and capecitabine, have already been registered. Both act through the dihydropyrimidine

[a]*Pharmacy, Cosmetic Chemistry and Biotechnology Research Group, Łukasiewicz Research Network-Industrial Chemistry Institute, Rydygiera 8, 01-793 Warsaw, Poland. E-mail: olga.michalak@ichp.lukasiewicz.gov.pl; marcin.cybulski@ichp.lukasiewicz.gov.pl; Tel: +48 453 056 175; +48 453 056 177*

[b]*Department of Lipids and Liposomes, Faculty of Biotechnology, University of Wroclaw, Fryderyka Joliot-Curie 14a, 50-383 Wroclaw, Poland*

[c]*Chemical and Biological Systems Simulation Laboratory, Center of New Technologies, University of Warsaw, Banacha 2c, 02-097 Warsaw, Poland*

[d]*Pharmaceutical Analysis Laboratory, Łukasiewicz Research Network-Industrial Chemistry Institute, Rydygiera 8, 01-793 Warsaw, Poland*

† Electronic supplementary information (ESI) available: Tables S1 and S2: ADMET properties of the tested compounds; synthesis of **18**, **26**, **28** and **29**; Fig. S1–S22 NMR spectra of **1–6**, **18**, **26**, **28**, **29**; Fig. S23–S28 HRMS spectra of **1–6**. See DOI: https://doi.org/10.1039/d4ra01683a

© 2024 The Author(s). Published by the Royal Society of Chemistry

Open Access Article. Published on 23 April 2024. Downloaded on 12/9/2025 12:17:06 AM.
This article is licensed under a Creative Commons Attribution-NonCommercial 3.0 Unported Licence.

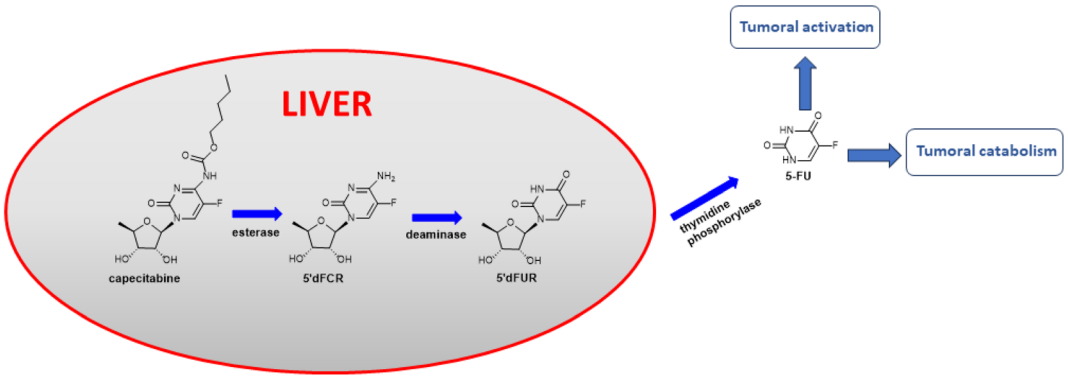

Fig. 1 Capecitabine metabolic pathway.[37]

dehydrogenase (DPD) inhibition mechanism. Capecitabine (brand name Xeloda) has been shown to be effective in treating colon, colorectal, gastric, and breast cancer in monotherapy. It may also be used with other cancer drugs, such as cisplatin, docetaxel, oxaliplatin, irinotecan or bevacizumab against gastric cancer, metastatic breast cancer[19] or metastatic colorectal cancer.[20] Various capecitabine derivatives have been designed and synthesized to date.[21,22] Recently, the PCC0208037 conjugate containing the haptophoric groups of irinotecan and capecitabine has been synthesized and evaluated *in vitro*.[23] Biological studies confirmed its anti-tumour activity and explored the potential molecular mechanism of action: cell cycle arrest and DNA damage. *In vivo* studies showed comparable anti-tumour efficacy of PCC0208037 in the xenograft colorectal cancer model and more favourable drug-like properties, as compared to irinotecan. Another ZRX1 conjugate acting as a prodrug of both the EGFR and the 5-FU inhibitor was also synthesized and biologically evaluated.[24] ZRX1 was designed to release 5-dFCR from its ester and the EGFR inhibitor in the first step of the metabolic pathway *via* hydrolysis by carboxylesterases (CES). The conjugate had the potential to induce a stronger growth inhibitory effect against human breast carcinoma cells than capecitabine or a single EGFR inhibitor and equivalent potency when compared with their combination.

Capecitabine (oral) and 5-FU (injection) are important drugs approved for the treatment of pancreatic cancer, either alone or in combination with FOLFIRINOX (folinic acid, fluorouracil, irinotecan, oxaliplatin) or OFF (oxaliplatin, fluorouracil, folinic acid) chemotherapy regimens.[25] Other mono- and combination therapies, such as paclitaxel nanoparticles, everolimus, erlotinib, gemcitabine, irinotecan liposomal, olaparib, mitomycin, and sunitinib, as well as gemcitabine with platinum compounds (cisplatin, oxaliplatin), have also not demonstrated significant benefits for pancreatic cancer treatment.[26–28]

Hydroxycinnamic acids have shown promising anticancer effects by inducing apoptosis through the modulation of intracellular reactive oxygen species (ROS).[29–32] Recently, intensive research on hydroxycinnamic acid derivatives has been focused in order to find new hybrid drugs.[33,34] Our previous results demonstrated that conjugates of indolo[2,3-*b*]quinoline antineoplastic with hydroxycinnamic acid analogues exhibit cytotoxic activity against primary AsPC-1 and metastatic BxPC-3 pancreatic cancer cells.[35] Furthermore, simple hydroxycinnamic acid analogues, when combined with curcumin and/or carnosic acid, exhibit synergistic activity against leukaemia cells.[36] One of the compounds in the metabolic pathway of capecitabine, to release active 5-FU, is 5′-deoxy-5-fluorocytidine 5-dFCR (Fig. 1). This compound is endogenously synthesized by hydrolysis of the amide group in capecitabine. Due to the presence of a free amino group in the chemical structure of 5-dFCR it was selected as a scaffold to design new group of its conjugates with hydroxycinnamic acids (HCA) by connection through amide-type bond.

The two predominant carboxylesterases CES1 and CES2 play a crucial role in the human body in the metabolism of a wide variety of esters.[38] CES2 prefers the hydrolysis of esters with a relatively large alcohol group and a small acyl group.[39] This characteristic was used in the successful design of prodrug compounds, in which biotransformation by CES2 is the first metabolic step to give an active drug, such as prasugrel, capecitabine, flutamide, and fluorescein diacetate. High CES2 activity in PDAC pancreatic ductal adenocarcinoma (*e.g.* BxPC-3, AsPC-1 cell lines) may be associated with the patient's increased sensitivity to irinotecan.[40,41] Moreover, elevated tumoral CES2 was a statistically significant predictor of poor overall survival in an orthotopic mouse model of PDAC.[42]

The systematic increase in cancer incidence combined with low survival rates in some types, including pancreatic cancer,[43] encourages the search for new effective molecules. Studies of conjugates of known chemotherapeutic drugs/or their prodrugs are one of the promising approaches to find compounds with an enhanced profile of action or better targeting known cancer pathways. As drug resistance limits the clinical utility of 5-FU, ROS modulation by phenolic compounds may be one method to overcome 5-FU resistance in cancer cells due to the different balance of ROS regulation in normal and cancer cells that affect their apoptosis mechanism.[44]

This work presents the synthesis, computational studies, and biological evaluation of new potential prodrugs **1–6** containing 5-dFCR and selected hydroxycinnamic acids in their structure (Fig. 2). The compounds were evaluated *in vitro* for

© 2024 The Author(s). Published by the Royal Society of Chemistry

Open Access Article. Published on 23 April 2024. Downloaded on 12/9/2025 12:17:06 AM.
This article is licensed under a Creative Commons Attribution-NonCommercial 3.0 Unported Licence.

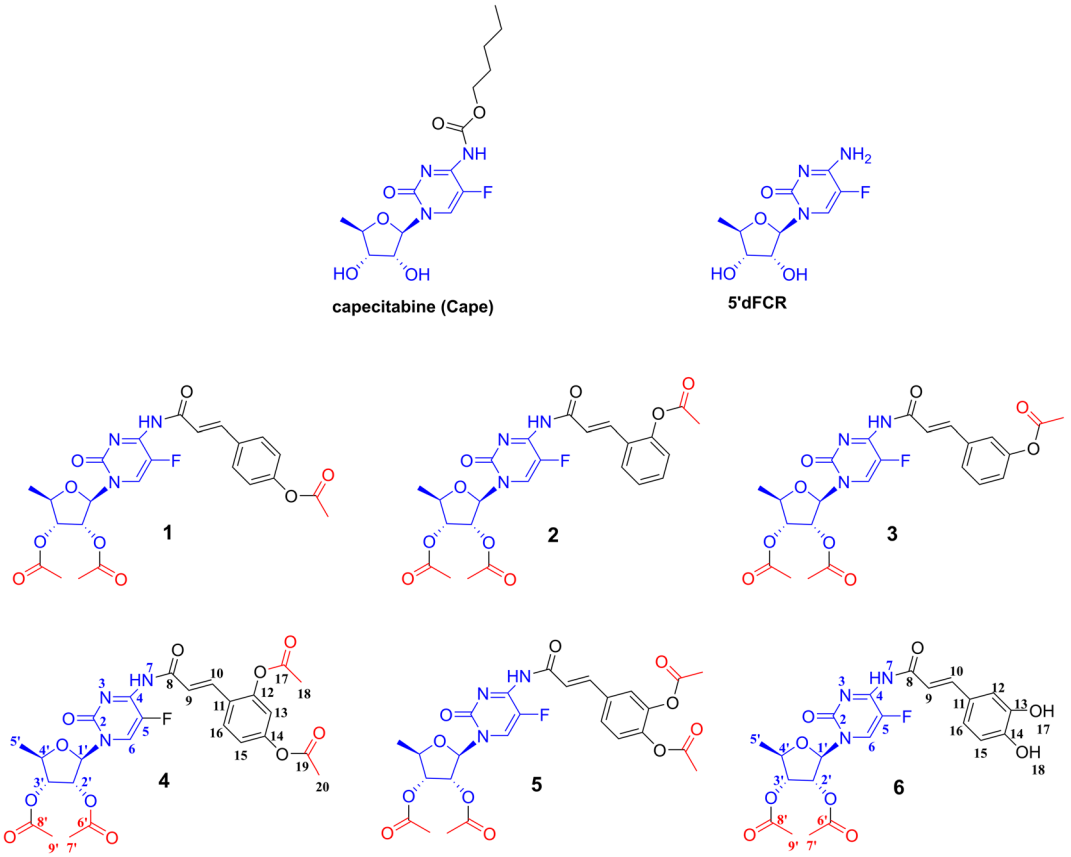

Fig. 2 Chemical structures of synthetised **1–6** prodrug conjugates of 5-dFCR and HCA.

their antiproliferative profile against pancreatic cancer cell lines. Cytotoxicity profiles were determined using the MTT assay. For the model compounds, **6** and its peracetylated precursor **5**, the difference in their potency on two PDAC cell lines related to the number of acetylated hydroxyl groups in their structures was discussed.

Results and discussion

Chemistry

Caffeic acid was selected as a typical substrate from the hydroxycinnamic acids group. The aim of the first set of experiments was to investigate the feasibility of synthesizing a model conjugate from 5-dFCR and caffeic acid. It was intended to obtain the dual molecule with all-free hydroxyl groups and connected by an amide bond. Due to the presence of phenolic-type hydroxyl groups, which are unstable at high pH[45] and also prone to oxidation, synthesis with unprotected phenolic acids as substrates is unfavourable. The HCA protection strategy may affect the effectiveness of the next coupling step. Therefore, it was decided to introduce various protecting groups to the hydroxyls of caffeic acid, to obtain stable coupling HCA substrates. Based on literature data,[46] three different protecting groups, which tolerate different deprotection conditions and stability, were selected for preliminary studies, that is, silyl,[47] acetyl[48] and allyl.[49] Similarly, the 5-dFCR substrate with isopropylidene or acetyl at the hydroxyl groups of the ribose ring was used for the syntheses. At first, di-*O*-protected silyl, acetyl, and allyl caffeic acid were synthesised according to known procedures.[50–52] Many methods of converting hydroxycinnamic acids to their corresponding amides by using classical reagents have been described in the literature. The classic HBTU/HOBt coupling of caffeic acid derivatives with L-serine methyl ester was described by Monteiro *et al.*[53] with the yields of 57–70%. Spasova *et al.*[54] used the EDCI/HOBt system to synthetise a group of hydroxycinnamic acid derivatives in order to study their antioxidant properties. A similar strategy was used by Takao[55] who obtained the suitable amides for antioxidant SAR studies. Rajan *et al.*[56] described the synthesis of amide hydroxycinnamic acids derivatives in the presence of BOP with a yield of 65–85%.

Thus, for our test reaction between caffeic acid and 5′-deoxy-5-fluoro-2′,3′-*O*-isopropylidenocytidine (**27**) PyBOP reagent was selected. Unfortunately, the TLC monitoring showed a complicated reaction mixture. After workup, the unreacted **27** was recovered with a yield of 70%. When EDCI/DMF reagent system was used, no cytidine derivative consumption was observed on TLC. Then, silyl-protected 3,4-di-*O*-*tert*-butyldimethylsilyl caffeic acid was reacted with 5′-deoxy-5-fluoro-2′,3′-*O*-isopropylidenocytidine (**27**) using various coupling agents: DCC, EDCI, TBTU, COMU. Due to ambiguous TLC results, the post-

Open Access Article. Published on 23 April 2024. Downloaded on 12/9/2025 12:17:06 AM.
This article is licensed under a Creative Commons Attribution-NonCommercial 3.0 Unported Licence.

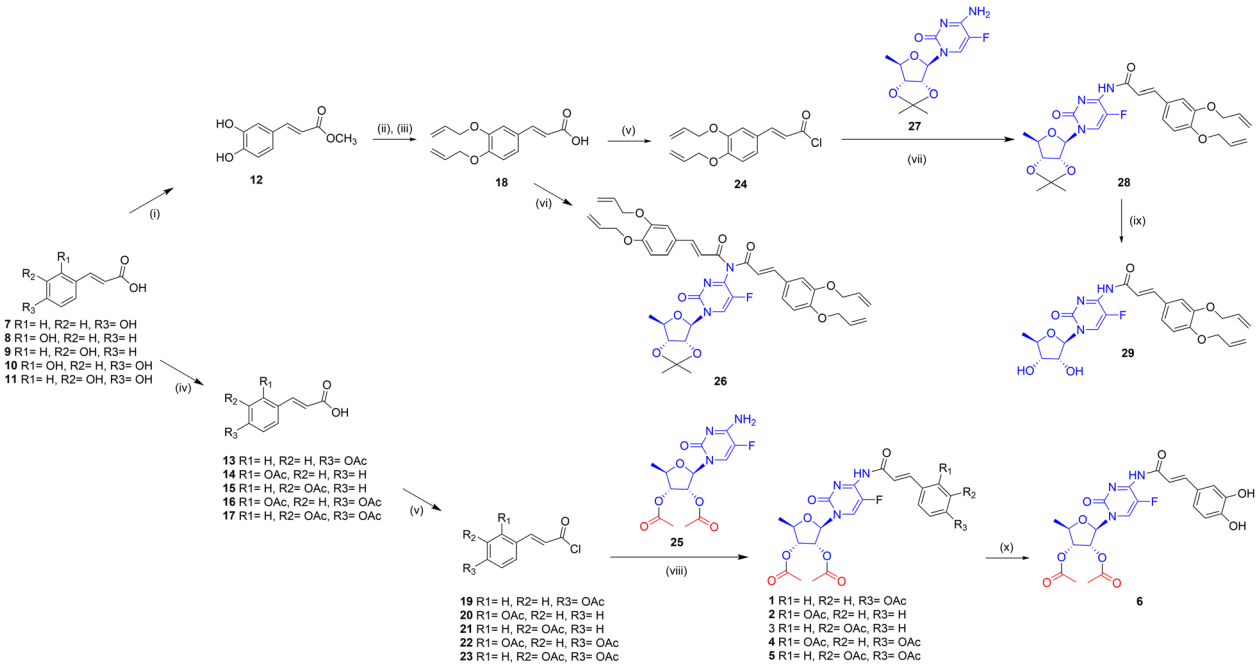

Fig. 3 Synthesis of **1–6**. Reagents and reaction conditions: (i) CH_3OH, CH_3COCl, r.t.; (ii) allyl bromide, K_2CO_3, acetone, r.t.; (iii) NaOH, H_2O/CH_3OH; (iv) pyridine, DMAP, $(CH_3CO)_2O$; (v) $SOCl_2$, DCM; (vi) $POCl_3$, pyridine; (vii) 50% NaOH aq./DCM; (viii) pyridine, DCM, −20 to −5 °C then r.t; (ix) 5 M HCl/MeOH; (x) K_2CO_3/chloroform.

reaction mixtures were purified using column chromatography to **27** as the main product.

Then, the relatively labile silyl groups were replaced with a stable allyl ether protection. Reaction with 3,4-di-*O*-allyl caffeic acid in the presence of COMU led to the activation of the carboxylic group. However, no further progress in amide formations was observed. In contrast, the reaction with PyBOP resulted in a complex mixture of TLC spots from various compounds, including a small spot from the anticipated amide product. Therefore, we decided to test the efficiency of carboxyl group activation through acid chlorides due to the small size of the leaving group.

At first, the protocol described by Quéléver *et al.*,[57] where acid chloride is generated *in situ* by $POCl_3$, was applied to give two reaction products: mono-**28** and disubstituted **26** derivatives of 5′-deoxy-5-fluoro-2′,3′-*O*-isopropylidenocytidine (Fig. 3). Despite the use of various molar excesses of the amine substrate, the reaction with $POCl_3$ gave the disubstituted derivative **26** as the main product. Since this observation, the allyl-protected acid **18** was transformed into the respective chloride **24** and conjugated with cytidine derivative **27** in the series of test reactions. The best reaction condition, that was, methylene chloride and 50% NaOH aqueous solvent, allowed to obtain the compound **28** in 91% yield. Experiments to remove allyl ethers from the completely protected derivative **28** were next carried out in the presence of tetrakis(-triphenylphosphine)palladium[49] ($Pd(PPh_3)_4$), or the DMSO-I_2 and DMSO-NaI reagent systems.[58–60] The attempts with Pd(0) catalyst led to a multispots reaction mixture on TLC plates. Reactions with iodine/iodide at room temperature showed no progress. However, when heated to 90 °C the cleavage of conjugates to the *O*-allyl-hydroxycinnamic acid was observed. For the reaction with tetrakis(triphenylphosphine)-palladium, the various solvents, including methanol or DMF, as well as different molar excesses of the catalyst were also verified. The results showed that the decomposition products, without a predominant compound, were detected on TLC. Reactions with palladium(II) chloride led to black suspensions containing the unreacted substrate with a lot of small impurities and a distinct tarry starting spot on TLC. Due to the unfavourable results of the removal of allyl from the compound with an isopropylidene protected sugar moiety, it was decided to change the sequence of deprotection. The isopropylidene removal was achieved in the single experiment by adding 5 M HCl in methanol to the crude post-reaction mixture of **28**. After 1 hour at ambient temperature, followed by extraction and chromatographic purification on silica gel compound **29** was isolated with a low yield of 23%.

We also investigated other conditions for removing the isopropylidene group, such as THF/1 M HCl or indium chloride in methanol. Unfortunately, these conditions resulted in substrate degradation without the expected product. Next, we attempted to remove the allyl groups from **29** using either the $Pd(PPh_3)_4$/MeOH/K_2CO_3 or $[Pd(P(C_6H_5)_3)_4]$/DCM system. However, the main product obtained was 5′-deoxy-5-fluorocytidine as a result of amide bond cleavage. Taking into consideration these results, it was decided to obtain the new peracetylated conjugates **1–6** as CES2 prodrugs. For this reason, the following substrates were synthesized: 5′-deoxy-2′,3′-di-*O*-acetyl-5-fluorocytidine (**25**) and *O*-acyl protected hydroxycinnamic acids **13–17**, all with yields greater than 90%. The coupling of **25** with **13–17** carried out in methylene chloride/50% NaOH aq., which was effective for **28**

© 2024 The Author(s). Published by the Royal Society of Chemistry

Open Access Article. Published on 23 April 2024. Downloaded on 12/9/2025 12:17:06 AM.
This article is licensed under a Creative Commons Attribution-NonCommercial 3.0 Unported Licence.

formations, did not yield products **1–5** and caused degradation of **13–17**. Finally, compounds **1–5** were obtained according to the procedure Shimma *et al.*,[61] by using methylene chloride with pyridine. Compound **5** was chosen as the model substrate for hydrolysis studies to remove acetyl groups. Various hydrolysis conditions were tested, including K_2CO_3 in methanol or 25% NH_3 aq. in methanol. The reaction progressed quickly, and several compounds were observed on TLC with no expected product or its traces. Only the reaction in chloroform and the presence of anhydrous K_2CO_3 produced the hydrolysis product. After purification on preparative TLC, we obtained conjugate **6** with a total yield of 42%. NMR analysis confirmed the structure of **6** and showed the absence of acetyl groups in the caffeic acid fragment of the conjugate. Compound **6**, which possesses two unbound hydroxyl groups, was tested to compare its *in vitro* activity with that of its peracetylated analogue **5**, and to determine the effect of the presence of CES2-sensitive ester groups on anti-PDAC activity.

In vitro anticancer activity against AsPC-1 and BxPC-3 pancreatic cancer lines and toxicity effect on normal human NHDF cells

The cytotoxic activity of conjugates **1–6** and the reference capecitabine (Cape) was tested using the MTT method adapted from Mosmann.[62] The compounds were dissolved in DMSO, diluted in culture medium to appropriate concentrations, and applied to metastatic AsPC-1 and primary BxPC-3 pancreatic cancer cells. After 72 hours of incubation, compounds showed similar moderate activity against AsPC-1 cancer cells in the IC_{50} range of 37–133 μM (Table 1, Fig. 4). Compound **6**, with unprotected hydroxyl groups in the caffeic acid fragment, showed the lowest activity towards AsPC-1 cells. All tested conjugates **1–6** exhibited significantly better activity against primary BxPC-3 pancreatic cancer cells compared to the metastatic line, with IC_{50} values ranging from 14–45 μM. Compound **4**, with a (2,4-diacetyloxy)cinnamoyl substituent, showed the lowest activity toward BxPC-3 cells, while compound **1**, with a *para*-(acetyloxy)coumaroyl substituent, showed the highest activity. It is worth emphasizing that peracetylated conjugate **5** and its simple analogue **6**, with unprotected hydroxyl groups in the caffeic acid part, exhibited similar activity against BxPC-3 cells (IC_{50} = 31.6 μM and 23.1 μM, respectively) and AsPC-1 cells (IC_{50} = 90.1 μM and 132.6 μM, respectively). However, peracetylated **5** was slightly more potent against AsPC-1 than semiacetylated conjugate **6**. The initial phase of *in vitro* research involves testing the compound on normal cell lines to confirm lower toxicity to healthy cells than to cancer cells, which is essential for identifying a potential clinical therapeutic window.[63] Therefore, we used normal human NHDF fibroblasts as model cells to evaluate the *in vitro* toxicity of conjugates **1–6**. All tested conjugates exhibited low selectivity towards the

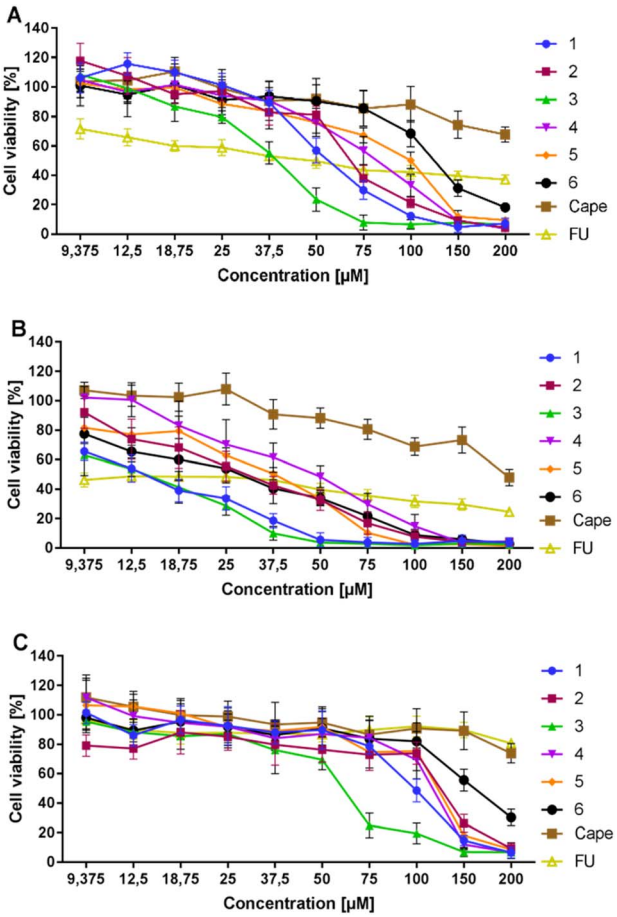

Fig. 4 Cytotoxic effects of **1–6** and capecitabine on AsPC-1 (A), BxPC-3 cells (B), and NHDF (C) expressed as % of viability compared to the untreated control.

Table 1 IC_{50} and selectivity index (SI) of **1–6** against PDAC lines measured by MTT assay[62]

	IC_{50} (μM)		IC_{50} (μM)	SI	
Compound	AsPC-1	BxPC-3	NHDF	AsPC-1	BxPC-3
1	57.15 ± 2.06	13.60 ± 2.48	96.49 ± 5.79	1.69	7.10
2	69.26 ± 4.00	26.93 ± 1.64	98.54 ± 10.46	1.42	3.66
3	37.00 ± 3.20	20.18 ± 2.43	60.04 ± 3.17	1.62	2.98
4	81.47 ± 3.60	45.09 ± 4.20	116.17 ± 2.71	1.43	2.58
5	90.07 ± 4.53	31.59 ± 0.82	121.30 ± 4.32	1.35	3.83
6	132.60 ± 5.67	23.16 ± 1.25	163.40 ± 4.33	1.23	7.06
Capecitabine (Cape)	>200	>200	>200	—	—
5-Fluorouracil (5-FU)	52.39 ± 11.56	12.74 ± 2.73	>200	—	—

© 2024 The Author(s). Published by the Royal Society of Chemistry

Open Access Article. Published on 23 April 2024. Downloaded on 12/9/2025 12:17:06 AM.
This article is licensed under a Creative Commons Attribution-NonCommercial 3.0 Unported Licence.

metastatic cell line, with a selectivity index (SI) between 1–2. However, the compounds acted more selectively in the case of the primary cell line BxPC-3. The caffeic acid derivative **6** and the *para*-coumaric acid derivative **1** showed the highest selectivity with an SI of approximately 7. The tests conducted on the PDAC lines did not reveal any significant differences in the activity of compounds **5** and **6**. This suggests that both compounds may undergo enzymatic hydrolysis to form the same active substance.

Computational studies

ADMET properties. To enhance the interpretation of ADME and docking results, we incorporated additional hypothetical structures **30–34** in the calculations (Fig. 5). These structures were structurally similar to the synthesised compounds **1–6**, but with two acetyl groups located in a different part of the molecule (compound **30**), all hydroxyl groups remaining free (compound **31**), and three phenolic-type hydroxyls (both free and acetylated, compounds **32–34**). The predicted ADMET properties of all compounds studied in this work are presented in Tables S1 and S2 in the ESI.† All compounds apart from **31** had at least one, and in most cases two violations of the Lipinski rule of five,[64] either due to the fact that they fall outside of the desired common limit of 500 Da that characterise systems with good oral bioavailability or have a large number of hydrogen bond donors/acceptors. However, these violations were minor and currently there have been many examples of drugs or drug candidates that violate these rules to a similar extent.[65] In the context of their potential toxicity, all compounds were predicted to be potential blockers of the HERG K+ channel, implicated in fatal arrhythmia,[66] although the obtained values were inconclusive. Predictions of toxicity using ProTox-II[67] revealed high estimated values of LD_{50} and no potential toxicity problems, similarly to capecitabine.

Docking studies. Molecular docking of the studied capecitabine to CES2 revealed two potential binding modes with crucial Ser228 interacting *via* a hydrogen bond with either the hydroxyl group or the amide group (Fig. 6). Compounds **1–6** were predicted to bind somewhat similarly to the first binding mode (site 1) of capecitabine with Ser228 interacting *via* a hydrogen bond with one of the acetate moieties connected to the deoxyribose moiety. Since Ser288 is part of the catalytic triad that catalyses the hydrolysis of ester groups, it was likely that in the case of compounds **1–6**, such hydrolysis may begin by interacting with this amino acid residue. Interestingly, derivatives **30**, **31** and **34** with acetate groups replaced by hydroxyl groups were predicted to bind in a very similar manner, as Ser228 was able to form hydrogen bonds also with these hydroxyl groups. However, in some cases, this binding was predicted to be weaker, lowering

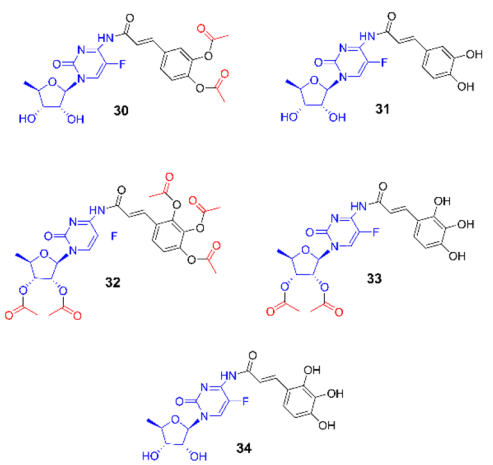

Fig. 5 Hypothetical structures of conjugates **30–34** used in computational studies.

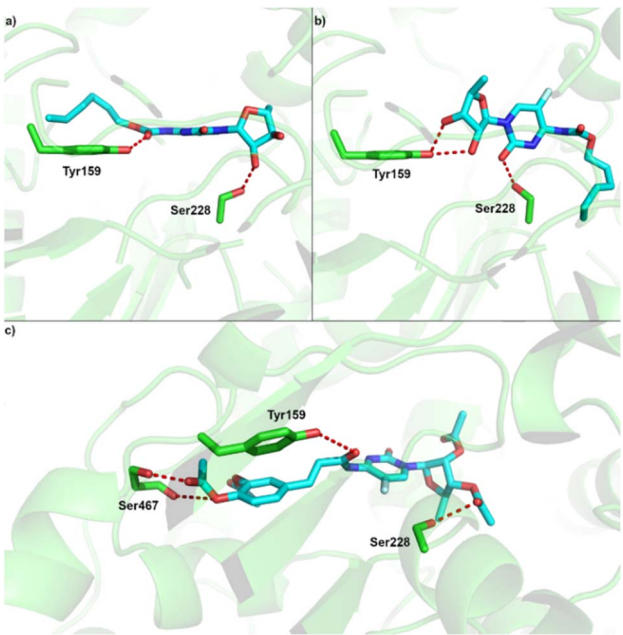

Fig. 6 Predicted binding site of CES2 and binding pose of (a) capecitabine (pose 1) (b) capecitabine (pose 2); (c) compound **5**.

Table 2 Predicted Gibbs free energies of binding and inhibition constants to CES2 for studied compounds

	Site 1	
Compound	ΔG^a (kcal mol^{-1})	$K_i{}^b$ (μm)
1	−12.1	0.001
2	−8.8	0.334
3	−12.1	0.001
4	−9.6	0.100
5	−11.7	0.002
6	−10.3	0.030
30	−10.8	0.013
31	−7.4	4.1
32	−5.2	143.1
33	−9.4	0.135
34	−6.7	13.1
5-dFCR	−7.5	5.0
Capecitabine	−7.6	4.0

[a] ΔG – Gibbs free energy of binding (in kcal mol^{-1}). [b] K_i – inhibition constant at 298 K (μm).

© 2024 The Author(s). Published by the Royal Society of Chemistry

Open Access Article. Published on 23 April 2024. Downloaded on 12/9/2025 12:17:06 AM.
This article is licensed under a Creative Commons Attribution-NonCommercial 3.0 Unported Licence.

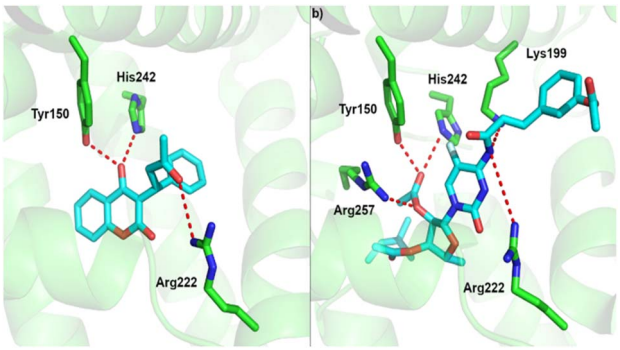

Fig. 7 Binding site of albumin and (a) experimental binding pose of warfarin and, (b) predicted binding pose of compound **3**.

Table 3 Predicted Gibbs free energies of binding and inhibition constants to albumin for studied compounds

	Site 1		Site 2	
Compound	ΔG^a (kcal mol^{-1})	K_i^b (μm)	ΔG (kcal mol^{-1})	K_i^b (μm)
1	−10.6	0.017	−9.5	0.107
2	−10.5	0.020	−7.9	1.601
3	−11.1	0.007	−7.6	2.658
4	−10.3	0.028	−8.9	0.296
5	−9.8	0.065	−9.3	0.150
6	−10.3	0.028	−8.0	1.353
30	−10.3	0.028	−8.0	1.353
31	−9.6	0.091	−7.8	1.896
32	−10.1	0.039	−7.6	2.658
33	−9.7	0.077	−8.5	0.581
34	−9.6	0.091	−7.7	2.245
5-dFCR	−7.2	5.224	−8.0	1.353
Capecitabine	−8.5	0.581	−8.0	1.353
Warfarin	−7.8	1.995	—	—

^{a} ΔG – Gibbs free energy of binding (in kcal mol^{-1}). ^{b} K_i – inhibition constant at 298 K (μm).

the overall Gibbs free binding energy and inhibition constants (Table 2). Additionally, for these compounds the catalytic triad of Ser228, Glu345 and His457 is predicted to be unable to perform its catalytic function due to the lack of ester moiety (which may be beneficial when no catalytic activity is desired). Furthermore, hypothetical compound **32** with five acetate substituents seemed to be too large to fit the catalytic site of CES2, resulting in a very weak binding to this site.

For albumin, we performed molecular docking of all studied compounds to the two potential binding sites, as predicted in previous work.[68] In all cases except 5-dFCR this computational approach predicts more favourable binding to site 1, which is also the native binding site of warfarin in the crystal structure of the warfarin-albumin complex.[69] Also, our computational protocol predicts that all compounds are bound substantially stronger to albumin than warfarin. The lowest inhibition constant value among all studied systems was predicted for compound **3** with low nanomolar value (Fig. 7, Table 3).

Conclusion

The new amide conjugates **1–6** of natural hydroxycinnamic acid (*ortho*-, *meta*-, *para*-coumaric, 2,4-dihydroxycinnamic, caffeic) and 5′-deoxy-5-fluorocytidine, the intermediate metabolite of oral capecitabine and prodrug of 5-fluorouracyl (5-FU), were obtained by evaluating different synthetic strategies. The most efficient method leading to peracetylated conjugates was the simple direct N-acylation of acetyl-protected 5′-deoxy-5-fluorocytidine with acetylated HCA acid chlorides. In *in vitro* studies, compounds **1–6** showed slightly higher efficacy against primary BxPC-3 than metastatic AsPC-1 pancreatic cancer cells with IC_{50} values ranging from 14–45 μM and 37–133 μM, respectively. They were also more selective in the case of the primary line, with the highest selectivity against normal dermal fibroblasts calculated to be about 7 for the caffeic acid derivative **6** and the *para*-coumaric acid derivative **1**. Considering that the compounds can act as substrates of CES2 carboxylesterase, we compared the *in vitro* activity of two compounds differing in the number of acetyl groups in the molecule, *i.e.* **5** and **6**. As a result, both showed similar activity against BxPC-3 cells with IC_{50} of 32 μM and 23 μM, and against AsPC-1 cells with IC_{50} of 90 μM and 133 μM, which may indicate the enzymatic hydrolysis of both compounds to the same active compound. Although the conjugates violated two of Lipinski's rules, related to molecular mass and number of hydrogen bonds, there are many examples of drugs or drug candidates that violate these rules to a similar extent. The toxicity predictions using ProTox-II showed high estimated LD_{50} values and no potential toxicity issues, similarly to capecitabine. Molecular docking to CES2 shows two potential binding modes with the critical Ser228. Compounds **1–6** were predicted to bind rather similarly to the binding mode of capecitabine and close to Ser228 from the catalytic triad, that catalysed the hydrolysis of ester groups. The strongest binding based on hydrogen bonding with acetyl group of sugar moieties was predicted for compounds **1**, **3** with K_i values of 0.001 μm and **5** with K_i value of 0.002 μm. Our computational protocol also estimated that all compounds bound significantly stronger to human serum albumin than warfarin, the most widely used oral anticoagulant. In summary, based on *in vitro* and *in silico* studies, compounds **1–6** could be viewed as potential lead structures for further modifications aimed at enhancing 5-FU activity against pancreatic cancer.

Experimental

For monitoring of reactions Merck DC-Alufolien Kieselgel 60 F25 TLC plates were used. Column chromatography was performed on Merck silica gel 60 (230–400 mesh). Melting points were measured on a Mettler Toledo MP90 apparatus and were uncorrected. NMR spectra were recorded on a Bruker AVANCE III HD 500 MHz spectrometer (at 298 K) in $CDCl_3$ and/or DMSO-d_6 using TMS as an internal standard. High-resolution mass spectrometry (HRMS) measurements were performed using Synapt G2-Si mass spectrometer (Waters) equipped with an ESI source and quadrupole-Time-of-Flight mass analyzer. The mass spectrometer operated in positive or negative ion detection modes. The measurement was performed with a capillary

Open Access Article. Published on 23 April 2024. Downloaded on 12/9/2025 12:17:06 AM. This article is licensed under a Creative Commons Attribution-NonCommercial 3.0 Unported Licence.

voltage set to 2.7 kV and a sampling cone set to 20 V. The source temperature was 110 °C. To ensure accurate mass measurements, the data was collected in centroid mode, and the mass was corrected during acquisition using leucine encephalin solution as an external reference, Lock-SprayTM, (Waters Corp., Milford, MA, USA), which generated a reference ion at *m*/*z* 554.2615 ($[M - H]^-$) in negative ESI mode and at *m*/*z* 556.2771 Da ($[M + H]^+$) in positive ESI mode. The results of the measurements were processed using the MassLynx 4.1 software (Waters).

MTT (3-(4,5-dimethylthiazol-2-yl)-2,5-diphenyltetrazolium bromide) were purchased from Sigma-Aldrich (Poznan, Poland) and DMSO from Archem (Kamieniec Wroclawski, Poland). Cell culture media (RPMI-1640, alpha-MEM and DMEM), stable glutamine 100×, trypsin–EDTA, heat inactivated fetal bovine serum premium (FBS) and antibiotic–antimycotic 100× were purchased from BioWest BioWest by CytoGen (Zgierz, Poland). The normal human dermal fibroblast cell line (NHDF) was purchased from Lonza (Lonza, Warsaw, Poland), and the BxPC-3 cell line was purchased from the American Tissue Culture Collection (ATCC, Manassas, VA, USA). The AsPC lines was kindly provided by the Institute of Immunology and Experimental Therapy (Wroclaw, Poland). The *trans*-hydroxycinnamic acids (HCA), 5′-deoxy-5-fluoro-2′,3′-*O*-isopropylidenocytidine (**27**, CAS 66335-37-3), 5′-deoxy-5-fluoro-2′,3′-di-*O*-acetylcytidine (**25**, CAS 161599-46-8), capecitabine (154361-50-9), chemical reagents and solvents were purchased from chemical suppliers. Acetyl protected HCA and methyl HCA esters were synthesized according to the common respective procedures.[48,70] Acetyl protected HCA were converted to the corresponding acid chlorides with an excess of thionyl chloride.

General procedure of synthesis of compounds 1–5

5′-Deoxy-5-fluoro-2′,3′-di-*O*-acetylcytidine (1 eq.) was dissolved in methylene chloride (4 mL) and dry pyridine (2 eq.) and cooled to −20 °C. To the stirred solution the respective hydroxycinnamoyl chloride (**19–23**) was added portionwise over a period of 15 min. with the temperature kept from −10 °C to −20 °C. The reaction was stirred 1 hour at −20 °C, then it was allowed to reach ambient temperature in 1 hour. After extraction in water/methylene chloride system, the separated organic layer was dried over anhydrous $MgSO_4$, and the solvent was distilled off under reduced pressure. Then crude product was purified using flash chromatography on silica gel.

2′,3′-Di-*O*-acetyl-5′-deoxy-5-fluoro-N^4-4-acetyloxycinnamoylcytidine (1)

Compound **1** was obtained as a white solid from 4-acetyloxycinnamoyl chloride **19** (0.17 g, 0.76 mM) and 5′-deoxy-5-fluoro-2′,3′-di-*O*-acetylcytidine (**25**) (0.25 g, 0.76 mM). The crude product (0.33 g) was purified by chromatography on a silica gel column with chloroform/methanol 50 : 1, followed by hexanes : ethyl acetate 1 : 2. Yield 0.11 g (28%); m.p. 79 °C (dec.).

^{1}H NMR (500 MHz, DMSO-d_6) δ 11.96 (d, 1H, J = 4.9 Hz, H-7, N*H*), 8.17 (d, 1H, J_{HF} = 6.9 Hz, H-6, double bond in flucytosine ring), 7.59 (d, 2H, J = 8.6 Hz, H-12, H-16, aromatic CA), 7.41 (d, 1H, J = 15.9 Hz, H-10, double bond CA), 7.16 (d, 2H, J = 8.6 Hz, H-13, H-15, aromatic CA), 6.57 (d, 1H, J = 15.9 Hz, H-9, double bond CA), 5.80 (d, 1H, J = 4.9 Hz, H-1′, C*H*N deoxyribose), 5.44 (dd, 1H, J_1 = 5.4 Hz, J_2 = 6.3 Hz, H-2′, deoxyribose), 5.08 (dd, 1H, $J_1 = J_2$ = 6.1 Hz, H-3′, deoxyribose), 4.07 (dq, 1H, $J_1 = J_2$ = 6.1 Hz, H-4′, deoxyribose), 2.27 (s, 3H, H-18, CH_3CO CA), 2.06 (s, 3H, H-9′, deoxyribose COCH_3), 2.04 (s, 3H, H-7′, CH_3CO deoxyribose), 1.34 (d, 3H, J = 6.3 Hz, H-5′, deoxyribose CH_3); ^{13}C NMR (125 MHz, DMSO-d_6) δ 169.5 (C-8′, deoxyribose *C*═O), 169.4 (C-6′, deoxyribose *C*═O), 169.1 (C-17, *C*═O CA), 166.6 (C-8, *C*═O CA), 157.0 (d, J_{2CF} = 26.2 Hz, C-4, flucytosine ring), 151.2 (C-14, aromatic CA), 149.0 (C-2, flucytosine ring *C*═O), 140.2 (d, J_{CF} = 231.6 Hz, C-5, flucytosine ring), 138.2 (C-10, double bond CA), 132.6 (C-11, aromatic CA), 128.7 (C-12, aromatic CA), 126.0 (d, J = 34.5 Hz, C-6, double bond), 122.4 (C-9, double bond CA), 122.4 (C-15, aromatic CA), 87.6 (C-1′, deoxyribose), 77.2 (C-4′, deoxyribose), 73.2 (C-3′, deoxyribose), 71.9 (C-2′, deoxyribose), 20.9 (C-18, *C*H$_3$CO CA), 20.3 (C-9′, deoxyribose COCH_3), 20.2 (C-7′, deoxyribose COCH_3), 17.9 (C-5′, deoxyribose *C*H$_3$); HRMS (ESI, *m*/*z*): calculated for $C_{24}H_{25}N_3O_9F$ $[M + H]^+$ 518.1575; found 518.1577, calculated for $C_{24}H_{24}N_3O_9FNa$ $[M + Na]^+$ 540.1394; found 540.1400.

2′,3′-Di-*O*-acetyl-5′-deoxy-5-fluoro-N^4-2-acetyloxycinnamoylcytidine (2)

Compound **2** was obtained as a white solid from 2-acetyloxycinnamoyl chloride **20** (0.17 g, 0.76 mM) and 5′-deoxy-5-fluoro-2′,3′-di-*O*-acetylcytidine (**25**) (0.25 g, 0.76 mM). The crude product (0.43 g) was purified by chromatography on a silica gel column with hexanes : ethyl acetate 1 : 2. Yield 0.17 g (42%); m.p. 74 °C (dec.).

^{1}H NMR (500 MHz, DMSO-d_6) δ 11.01 (bs, 1H, H-7, N*H*), 8.40 (bs, 1H, H-6, double bond in flucytosine ring), 7.75 (d, 1H, J = 6.9 Hz, H-16, aromatic CA), 7.61 (d, 1H, J = 15.9 Hz, H-10, double bond), 7.49 (m, 1H, H-14, aromatic CA), 7.36 (dd, 1H, $J_1 = J_2$ = 7.5 Hz, H-15, aromatic CA), 7.24 (d, 1H, J = 8.0 Hz, H-13, aromatic CA), 7.14 (d, 1H, J = 15.4 Hz, H-9, double bond), 5.83 (d, 1H, J = 4,1 Hz, H-1′, C*H*N deoxyribose), 5.49 (dd, 1H, J_1 = 4.2 Hz, J_2 = 6.2 Hz, H-2′, deoxyribose), 5.13 (dd, 1H, $J_1 = J_2$ = 6.4 Hz, H-3′, deoxyribose), 4.14 (dq, 1H, $J_1 = J_2$ = 6.4 Hz, H-4′, deoxyribose), 2.37 (s, 3H, H-18, CH_3CO CA), 2.06 (s, 3H, H-9′, deoxyribose COCH_3), 2.06 (s, 3H, H-7′, deoxyribose COCH_3), 1.37 (d, 3H, J = 6,3 Hz, H-5′, deoxyribose CH_3); ^{13}C NMR (125 MHz, DMSO-d_6) δ 169.5 (C-8′, deoxyribose *C*═O), 169.3 (C-6′, deoxyribose *C*═O), 169.2 (C-17, *C*═O CA), 163.8 (C-8, *C*═O CA), 154.5 (C-4, flucytosine ring), 152.3 (C-2, flucytosine ring *C*═O), 149.2 (C-12, aromatic CA), 137.5 (d, C-5, flucytosine ring), 136.4 (C-10, double bond CA), 131.6 (C-6, flucytosine ring), 131.4 (C-14, aromatic CA), 128.2 (C-16, aromatic CA), 126.8 (C-11, aromatic CA), 126.6 (C-15, aromatic CA), 123.6 (C-13, aromatic CA), 122.9 (C-9, double bond CA), 90.00 (C-1′, deoxyribose), 77.4 (C-4′, deoxyribose), 73.4 (C-3′, deoxyribose), 72.7 (C-2′, deoxyribose), 20.7 (C-18, *C*H$_3$CO CA), 20.3 (C-9′, deoxyribose COCH_3), 20.3 (C-7′, deoxyribose COCH_3), 17.7 (C-5′, deoxyribose *C*H$_3$); HRMS (ESI, *m*/*z*): calculated for $C_{24}H_{25}N_3O_9F$ $[M + H]^+$ 518.1575; found 518.1580, calculated for $C_{24}H_{24}N_3O_9FNa$ $[M + Na]^+$ 540.1394; found 540.1398.

© 2024 The Author(s). Published by the Royal Society of Chemistry

Open Access Article. Published on 23 April 2024. Downloaded on 12/9/2025 12:17:06 AM. This article is licensed under a Creative Commons Attribution-NonCommercial 3.0 Unported Licence.

2′,3′-Di-*O*-acetyl-5′-deoxy-5-fluoro-N^4-3-acetyloxycinnamoyl-cytidine (3)

Compound **3** was obtained as a white solid from 3-acetyloxycinnamoyl chloride **21** (0.17 g, 0.76 mM) and 5′-deoxy-5-fluoro-2′,3′-di-*O*-acetylcytidine (**25**) (0.25 g, 0.76 mM). The crude product (0.33 g) was purified by chromatography on a silica gel column with chloroform/methanol 50 : 1, followed by hexanes : ethyl acetate 1 : 2. Yield 0.16 g (40%); m.p. 75 °C (dec.).

^{1}H NMR (500 MHz, DMSO-d_6) δ 11.96 (d, 1H, J = 4,9 Hz, H-7, N*H*), 8.17 (d, 1H, J = 6.9 Hz, H-6, double bond in flucytosine ring), 7.44 (m, 1H, H-15, aromatic CA), 7.44 (m, 1H, H-12, aromatic CA), 7.39 (d, 1H, J = 15.9 Hz, H-10, double bond CA), 7.32 (m, 1H, H-16, aromatic CA), 7.13 (m, 1H, H-14, aromatic CA), 6.61 (d, 1H, J = 15.9 Hz, H-9, double bond CA), 5.80 (d, 1H, J = 5.1 Hz, H-1′, C*H*N deoxyribose), 5.44 (dd, 1H, J_1 = 5.6 Hz, J_2 = 6.1 Hz, H-2′, deoxyribose), 5.08 (dd, 1H, J_1 = J_2 = 6.1 Hz, H-3′, deoxyribose), 4.07 (dq, 1H, J_1 = J_2 = 6.1 Hz, H-4′, deoxyribose), 2.27 (s, 3H, H-18, C*H*$_3$CO CA), 2.06 (s, 3H, H-9′, deoxyribose COC*H*$_3$), 2.04 (s, 3H, H-7′, deoxyribose COC*H*$_3$), 1.35 (d, 1H, J = 6.3 Hz, H-5′, deoxyribose C*H*$_3$); ^{13}C NMR (125 MHz, DMSO-d_6) δ 169.5 (C-8′, deoxyribose *C*=O), 169.4 (C-6′, deoxyribose *C*=O), 169.2 (C-17, *C*=O CA), 166.4 (C-8, *C*=O CA), 157.0 (d, J = 26.0 Hz, C-4, flucytosine ring), 150.9 (C-13, aromatic CA), 149.0 (C-2, flucytosine ring *C*=O), 140.2 (d, J = 231.6 Hz, C-5, flucytosine ring), 138.1 (C-10, double bond CA), 136.5 (C-11, aromatic CA), 130.0 (C-15, aromatic CA), 126.0 (d, J = 34.4 Hz, C-6, flucytosine ring), 125.1 (C-12, aromatic CA), 123.4 (C-9, double bond CA), 122.8 (C-14, aromatic CA), 120.5 (C-16, aromatic CA), 87.6 (C-1′, deoxyribose), 77.2 (C-4′, deoxyribose), 73.2 (C-3′, deoxyribose), 71.9 (C-2′, deoxyribose), 20.8 (C-18, *C*H$_3$CO CA), 20.3 (C-9′, deoxyribose COC*H*$_3$), 20.2 (C-7′, deoxyribose COC*H*$_3$), 17.9 (C-5′, deoxyribose *C*H$_3$); HRMS (ESI, *m*/*z*): calculated for $C_{24}H_{25}N_3O_9F$ $[M + H]^+$ 518.1575; found 518.1579, calculated for $C_{24}H_{24}N_3O_9FNa$ $[M + Na]^+$ 540.1394; found 540.1398.

2′,3′-Di-*O*-acetyl-5′-deoxy-5-fluoro-N^4-2,4-acetyloxycinnamoyl-cytidine (4)

Compound **4** was obtained as a white solid from 2,4-diacetyloxycinnamoyl chloride **22** (0.13 g, 0.46 mM) and 5′-deoxy-5-fluoro-2′,3′-di-*O*-acetylcytidine (**25**) (0.15 g, 0.46 mM). The crude product (0.21 g) was purified by chromatography on a silica gel column with hexanes : ethyl acetate : methanol 5 : 5:1. Yield 0.1 g (38%); m.p. 96 °C (dec.).

^{1}H NMR (500 MHz, DMSO-d_6) δ 11.04 (bs, 1H, H-7, NH), 8.39 (bs, 1H, H-6, double bond in flucytosine ring), 7.79 (d, 1H, J = 7.6 Hz, H-16, aromatic CA), 7.59 (d, 1H, J = 15.9 Hz, H-10, double bond CA), 7.17 (m, 1H, H-15, aromatic CA), 7.14 (m, 1H, H-13, aromatic CA), 7.11 (m, 1H, H-9, double bond CA), 5.83 (d, 1H, J = 4.0 Hz, H-1′, C*H*N deoxyribose), 5.49 (dd, 1H, J_1 = 4.5 Hz, J_2 = 6.1 Hz, H-2′, deoxyribose), 5.13 (dd, 1H, J_1 = J_2 = 6.4 Hz, H-3′, deoxyribose), 4.13 (dq, 1H, J_1 = J_2 = 6.3 Hz, H-4′, deoxyribose), 2.37 (s, 3H, H-18, C*H*$_3$CO CA), 2.28 (s, 3H, H-20, C*H*$_3$CO CA), 2.06 (s, 3H, H-9′, deoxyribose COC*H*$_3$), 2.06 (s, 3H, H-7′, deoxyribose COC*H*$_3$), 1.37 (d, 1H, J = 6.3 Hz, H-5′, deoxyribose C*H*$_3$); ^{13}C NMR (125 MHz, DMSO-d_6) δ 169.5 (C-8′, deoxyribose *C*=O), 169.3 (C-6′, deoxyribose *C*=O), 168.9 (C-17, *C*=O CA), 168.8 (C-19, *C*=O CA), 163.9 (C-8, *C*=O CA), 154.5 (C-4, flucytosine ring), 152.2 (C-2, flucytosine ring *C*=O), 152.1 (C-14, aromatic CA), 149.6 (C-12, aromatic CA), 137.5 (d, C-5, flucytosine ring), 135.7 (C-10, double bond CA), 131.4 (C-6, flucytosine ring), 129.00 (C-16, aromatic CA), 124.5 (C-11, aromatic CA), 123.0 (C-9, double bond CA), 120.3 (C-15, aromatic CA), 117.4 (C-13, aromatic CA), 89.9 (C-1′, deoxyribose), 77.4 (C-4′, deoxyribose), 73.4 (C-3′, deoxyribose), 72.7 (C-2′, deoxyribose), 20.8 (C-20, *C*H$_3$CO CA), 20.7 (C-18, *C*H$_3$CO CA), 20.3 (C-9′, deoxyribose COC*H*$_3$), 20.3 (C-7′, deoxyribose COC*H*$_3$), 17.7 (C-5′, deoxyribose *C*H$_3$); HRMS (ESI, *m*/*z*): calculated for $C_{26}H_{27}N_3O_{11}F$ $[M + H]^+$ 576.1630; found 576.1631, calculated for $C_{26}H_{26}N_3O_{11}FNa$ $[M + Na]^+$ 598.1449; found 598.1451.

2′,3′-Di-*O*-acetyl-5′-deoxy-5-fluoro-N^4-3,4-diacetyloxycinnamoyl-cytidine (5)

Compound **5** was obtained as a white solid from 3,4-diacetyloxycinnamoyl chloride **23** (0.86 g, 3.04 mM) and 5′-deoxy-5-fluoro-2′,3′-di-*O*-acetylcytidine (**25**) (1.00 g, 3.04 mM). The crude product (1.69 g) was purified by chromatography on a silica gel column with chloroform/methanol 50 : 1, followed by hexanes : ethyl acetate : methanol 5 : 5 : 1. Yield 0.85 g (49%); m.p. 88 °C (dec.).

^{1}H NMR (500 MHz, $CDCl_3$) δ 7.84 (d, 1H, J = 15.7 Hz, H-10, double bond), 7.53 (s, 1H, H-7, N*H*), 7.49 (d, 1H, J = 8.5 Hz, H-16, aromatic CA), 7.42 (d, 1H, J = 1.8 Hz, H-12, aromatic CA), 7.23 (d, 1H, J = 8.5 Hz, H-15, aromatic CA), 5.98 (d, 1H, J = 4.6 Hz, H-1′, C*H*N deoxyribose), 5.32 (dd, J_1 = J_2 = 5.1 Hz, H-2′, deoxyribose), 5.01 (dd, J_1 = J_2 = 5.7 Hz, H-3′, deoxyribose), 4.27 (dq, 1H, J_1 = J_2 = 6.1 Hz, H-4′, deoxyribose), 2.30 (s, 3H, H-20, C*H*$_3$CO CA), 2.29 (s, 3H, H-18, C*H*$_3$CO CA), 2.11 (s, 3H, H-7′, deoxyribose COC*H*$_3$), 2.10 (s, 3H, H-9′, deoxyribose COC*H*$_3$), 1.48 (d, 3H, J = 6.4 Hz, H-5′, deoxyribose C*H*$_3$); ^{13}C NMR (125 MHz, $CDCl_3$) δ 169.7 (C-8′, *C*=O deoxyribose), 169.6 (C-6′, *C*=O deoxyribose), 168.0 (C-17, *C*=O CA), 167.9 (C-19, *C*=O deoxyribose), 152.4 (C-2, C=O flucytosine ring), 144.0 (C-10, double bond), 143.6 (C-14, aromatic CA), 142.4 (C-13, aromatic CA), 133.5 (C-11, aromatic CA), 126.8 (C-16, aromatic CA), 123.9 (C-15, aromatic CA), 123.3 (C-12, aromatic CA), 88.4 (C-1′, deoxyribose *C*H), 78.2 (C-4′, deoxyribose), 73.9 (C-3′, deoxyribose), 73.3 (C-2′, deoxyribose), 20.6 (C-18, *C*H$_3$CO CA), 20.6 (C-20, *C*H$_3$CO CA), 20.5 (C-9′, deoxyribose COC*H*$_3$), 20.4 (C-7′, deoxyribose COC*H*$_3$), 18.7 (C-5′, deoxyribose *C*H$_3$).

^{1}H NMR (500 MHz, DMSO-d_6) δ 11.96 (d, 1H, J = 5.0 Hz, H-7, N*H*), 8.17 (d, 1H, J = 6.9 Hz, H-6, double bond in flucytosine ring), 7.49 (m, 1H, H-16, aromatic CA), 7.47 (m, 1H, H-12, aromatic CA), 7.39 (d, 1H, J = 15.9 Hz, H-10, double bond CA), 7.30 (d, 1H, J = 8.3 Hz, H-15, aromatic CA), 6.68 (d, 1H, J = 15.9 Hz, H-9, double bond CA), 5.80 (d, 1H, J = 5,2 Hz, H-1′, C*H*N deoxyribose), 5.43 (dd, 1H, J_1 = 5.3 Hz, J_2 = 6.3 Hz, H-2′, deoxyribose), 5.08 (dd, 1H, J_1 = J_2 = 6.1 Hz, H-3′, deoxyribose), 4.07 (dq, 1H, J_1 = J_2 = 6.1 Hz, H-4′, deoxyribose), 2.28 (s, 6H, H-18, H-20, C*H*$_3$CO CA), 2.06 (s, 3H, H-9′, deoxyribose COC*H*$_3$), 2.04 (s, 3H, H-7′, deoxyribose COC*H*$_3$), 1.34 (d, 3H, J = 6.3 Hz, 3H, H-5′, deoxyribose C*H*$_3$); ^{13}C NMR (125 MHz, DMSO-d_6) δ 169.5 (C-8′, deoxyribose *C*=O), 169.4 (C-6′, deoxyribose *C*=O), 168.2 (C-19,

Open Access Article. Published on 23 April 2024. Downloaded on 12/9/2025 12:17:06 AM. This article is licensed under a Creative Commons Attribution-NonCommercial 3.0 Unported Licence.

C=O CA), 168.2 (C-17, *C*=O CA), 166.35 (C-8, *C*=O CA), 157.0 (d, $J = 26.1$ Hz, C-4, flucytosine ring), 149.0 (C-2, flucytosine ring *C*=O), 142.7 (C-14, aromatic CA), 142.3 (C-13, aromatic CA), 140.2 (d, $J_{CF} = 231.6$ Hz, C-5, flucytosine ring), 137.5 (C-10, double bond CA), 133.8 (C-11, aromatic CA), 126.0 (d, $J = 33.7$ Hz, C-6, flucytosine ring), 124.1 (C-15, aromatic CA), 123.4 (C-9, double bond CA), 122.3 (C-12, aromatic CA), 87.6 (C-1′, deoxyribose), 77.2 (C-4′, deoxyribose), 73.2 (C-3′, deoxyribose), 71.9 (C-2′, deoxyribose) 20.3 (C-18, CH_3CO CA), 20.3 (C-20, CH_3CO CA), 20.3 (C-9′, deoxyribose $COCH_3$), 20.2 (C-7′, deoxyribose $COCH_3$), 17.9 (C-5′, deoxyribose CH_3); HRMS (ESI, *m*/*z*): calculated for $C_{26}H_{27}N_3O_{11}F$ $[M + H]^+$ 576.1630; found 576.1633, calculated for $C_{26}H_{26}N_3O_{11}FNa$ $[M + Na]^+$ 598.1449; found 598.1448.

2′,3′-Di-*O*-acetyl-5′-deoxy-5-fluoro-N^4-3,4-dihydroxycinnamoyl-cytidine (6)

To 2′,3′-di-*O*-acetyl-5′-deoxy-5-fluoro-N^4-3,4-diacetyloxycinnamoyl-cytidine **5** (0.15 g; 0.261 mmol) in methylene chloride (6.5 mL), anhydrous potassium carbonate (0.269 g; 0.339 mmol) was added. The reaction mixture was stirred overnight and then filtered. The precipitate was washed with methylene chloride, then ethyl acetate. Next it was dissolved in water, acidified to pH = 5 using 0.5 M HCl aq. and extracted with ethyl acetate (3 × 20 mL). The combined organic fractions were dried over anhydrous $MgSO_4$, and the solvent was distilled off under reduced pressure The crude product (0.113 mg) was purified using flash column chromatography on a silica gel with chloroform: methanol 95 : 5 to 9 : 1, then on a preparative TLC plate/SiO_2/1 mm with chloroform : methanol 95 : 5. After evaporation to oil, the compound **6** was precipitated off using ethyl acetate/*n*-hexane mixture to give 6 as a yellow solid. Yield 0.054 g (42%); m.p. 116 °C (dec.); ^{1}H NMR (500 MHz, DMSO-d_6) δ 10.73 (s, 1H, H-7, N*H*), 9.59 (s, 1H, H-17, phenolic O*H*), 9.25 (s, 1H, H-18, phenolic O*H*), 8.37 (d, 1H, $J = 4.7$ Hz, H-6, double bound in flucytosine ring), 7.50 (d, 1H, $J = 15.6$ Hz, H-10, double bound), 7.03 (d, 1H, $J = 1.9$ Hz, H-12, aromatic CA), 6.95 (dd, 1H, $J_1 = 8.2$ Hz, $J_2 = 1.7$ Hz, H-16, aromatic CA), 6.84 (d, 1H, $J = 15.4$ Hz, H-9, double bond), 6.78 (d, 1H, $J = 8.2$ Hz, H-15, aromatic CA), 5.82 (d, 1H, $J = 4.2$ Hz, H-1′, C*H*N deoxyribose), 5.49 (dd, 1H, $J_1 = 6.2$ Hz, $J_2 = 4.3$ Hz, H-2′, deoxyribose), 5.13 (dd, 1H, $J_1 = J_2 = 6.4$ Hz, H-3′, deoxyribose), 4.13 (dt, $J_1 = J_2 = 6.3$ Hz, H-4′, deoxyribose) 2.06 (s, 6H, H-7′, H-9′, deoxyribose C(O)CH_3), 1.37 (d, 3H, $J = 6.3$ Hz, H-5′, deoxyribose CH_3), ^{13}C NMR (125 MHz, DMSO-d_6) δ 169.5 (C-8′, deoxyribose *C*=O), 169.3 (C-6′, deoxyribose *C*=O), 164.3 (C-8, *C*=O CA), 154.6 (C-4, flucytosine ring), 152.3 (C-2, flucytosine ring *C*=O), 148.6 (C-14, aromatic CA), 145.6 (C-13, aromatic CA), 144.2 (C-10, double bond), 137.3 (d, $J_{CF} = 247.1$ Hz, C-5, flucytosine ring), 131.3 (d, $J_{CF} = 36.0$ Hz, C-6, flucytosine ring), 125.8 (C-11, aromatic CA), 121.8 (C-16, aromatic CA), 116.6 (C-9, double bond), 115.8 (C-15, aromatic CA), 114.2 (C-12, aromatic CA), 89.9 (C-1′, deoxyribose), 77.3 (C-4′, deoxyribose), 73.4 (C-3′, deoxyribose), 72.7 (C-2′, deoxyribose), 20.3 (C-7′, deoxyribose $COCH_3$), 20.3 (C-9′, deoxyribose $COCH_3$), 17.7 (C-5′, deoxyribose CH_3); HRMS (ESI, *m*/*z*): calculated for $C_{22}H_{23}N_3O_9F$ $[M + H]^+$ 492.1418; found 492.1418, calculated for $C_{22}H_{22}N_3O_9FNa$ $[M + Na]^+$ 514.1238; found 514.1234.

Cell culture

In vitro cell culture procedures were performed under aseptic conditions and cells were propagated in humidified Innova CO-180 incubator (New Brunswick Scientific, Edison, NJ, USA) supplied with 5% CO_2 and maintained at 37 °C. Subculturing was performed twice per week (at approximately 72 h intervals) and cell growth was monitored with a Nikon Eclipse microscope. Pancreatic cancer cell lines: BxPC-3 (from primary tumour) and AsPC-1 (from ascites) were cultured in RPMI-1640 medium supplemented with 10% heat inactivated fetal bovine serum (FBS), glutamine and antibiotic–antimycotic mixture. NHDF grew in alpha-MEM supplemented with 10% FBS, 2 mM glutamine, and antibiotic–antimycotic.

Cell viability assay (MTT)

The cytotoxicity impact of the ligands on cancer cell and healthy control cell lines was evaluated as described earlier[71–73] by performing the MTT assay.[62] Cells were seeded in 96-well plates (at a density of 5×10^3 cells per well) in appropriate culture medium and plates were incubated for 24 h. Afterwards, the media were replaced with fresh media supplemented with varying concentration (in the range of 125–4000 nM) of synthesized complexes (compounds were dissolved in DMSO, heated and sonicated at 55 °C for 15 min before dilution in medium) or an equivalent volume of DMSO, considered as solvent control and incubation proceeded for another 72 h. Subsequently, the medium containing the chemicals tested was removed and the MTT solution (50 μL per well of 10 times diluted in medium from the solution stock 0.5 mg mL^{-1}) was added. After 3 h of incubation, the MTT solution was replaced with DMSO (50 μL per well) to dissolve the purple formazan crystals and developed color. Absorbance was measured at 560 nm with a reference wavelength of 670 nm on an Asys UVM 340 Microplate Reader (Cambridge, UK). The results were expressed as a percentage of viable cells in comparison to the control (the untreated cells, taken as 100%) implementing the formula:

$$\text{Cell viability (\%)} = (\text{AT/AC}) \times 100$$

where, AT = absorbance of the treated cells, AC = absorbance of the not treated cells.

Computational methods

In the computational part of this work, we used a similar approach to our previous studies.[74–76] Models of all studied ligands were built starting from the structure of capecitabine (Pubchem CID: 60953).[77] LigProp 3.3 software (Schrodinger Inc.) was used to prepare all-atom 3D structures. Subsequently, we evaluated all ADME properties using QikProp 4.6 software (Schrodinger Inc.) with default options. For the toxicity prediction, we used ProTox-II webserver.[67] In the molecular docking part, we used Autodock Vina ver. 1.1.2 (ref. 78) with default options and exhaustiveness level set at 18. For molecular docking to CES2, we used the AlphaFold model of this protein.[79] with the following residues set as flexible: Trp145, Tyr159,

© 2024 The Author(s). Published by the Royal Society of Chemistry

Open Access Article. Published on 23 April 2024. Downloaded on 12/9/2025 12:17:06 AM.
This article is licensed under a Creative Commons Attribution-NonCommercial 3.0 Unported Licence.

Glu227, Ser228, Thr232, Ser233, Ser235, Leu259, Phe416, His457, Glu460, Leu461. After the docking we selected the lowest-energy pose of ligand **5** and used it as a template to build all other ligand models, which were redocked to the protein using Autodock ver. 4.2 (ref. 80) and the local search algorithm with 1000 repetitions. For albumin docking we used the available crystal structure of this protein (PDB: 2BXD)[69] and two potential binding sites, as predicted in previous studies.[68] For site 1 the following residues were treated as flexible: Tyr150, Lys199, Phe211, Arg222, Leu238, His242, Arg257, Leu260, while for site 2 the flexible residues were: Leu387, Asn391, Arg410, Tyr411, Lys414, Arg485, Ser489. In both cases we used a 25 × 25 × 25 Å box centered on the corresponding binding sites.

Author contributions

Conceptualization, M. C. and O. M.; methodology, M. C., M. Z.-C., A. J., P. K., and B. T.; software, B. T.; formal analysis, B. T. and M. Z.-C.; investigation, M. C., J. T., M. Z.-C., P. K., B. T. and M. K.; resources, M. C., M. Z.-C., B.·K., A. J. and O. M.; data curation, B. T., M. K., M. Z.-C.; writing—original draft preparation, M. C. and B. T.; writing—review and editing, M. C., M. Z.-C., O. M. and B. T.; visualization, M. C., M. Z.-C. and B. T.; supervision, M. C., P. K. M. K., A. J. and O. M.; project administration, M. C. and O. M.; funding acquisition, M. C. and O. M. All authors have read and agreed to the published version of the manuscript.

Conflicts of interest

There are no conflicts to declare.

Acknowledgements

This research was funded by Łukasiewicz Center, grant agreement no. 4/Ł-ICHP/CŁ/2021. Authors wish to acknowledge our colleagues: Katarzyna Sidoryk (Pikralida sp. z o.o, Poland) and Sylwia Żelazowska (Łukasiewicz Research Network–Industrial Chemistry Institute, Warsaw, Poland) for scientific comments and NMR data entry.

References

1 R. Mokhtari, T. Homayouni, N. Baluch, E. Morgatskaya, S. Kumar, B. Das and H. Yeger, *Oncotarget*, 2017, **8**(23), 38022.
2 M. Kudo, *World J. Gastroenterol.*, 2019, **25**(7), 789.
3 A. Eras, D. Castillo, M. Suárez, N. Vispo, F. Albericio and H. Rodriguez, *Front. Chem.*, 2022, **10**, 889083.
4 M. Szumilak, A. Wiktorowska-Owczarek and A. Stanczak, *Molecules*, 2021, **26**(9), 2601.
5 K. Tkaczuk, *Clin. Ther.*, 2009, **31**(2), 2273.
6 A. VanHook, *Sci. Signaling*, 2014, **7**(347), 284.
7 Y. Lee, K. Bae, H. Yoo and S. Cho, *Integr. Cancer Ther.*, 2018, **17**, 619.
8 S. Kamran, A. Sinniah, Z. Chik and M. Alshawsh, *Biomedicines*, 2022, **10**(3), 531.
9 A. Palmer, B. Izar, H. Hwangbo and P. Sorger, *Clin. Cancer Res.*, 2022, **28**(2), 368.
10 B. Fox, X. Xiao, S. Antony, G. Kohlhagen, Y. Pommier, B. Staker, L. Stewart and M. Cushman, *J. Med. Chem.*, 2003, **46**(15), 3275.
11 K. Sashidhara, A. Kumar, M. Kumar, J. Sarkar and S. Sinha, *Bioorg. Med. Chem. Lett.*, 2010, **20**(24), 7205.
12 L. Zhang and Z. Xu, *Eur. J. Med. Chem.*, 2019, **181**, 111587.
13 C. do Pazo, K. Nawaz and M. Webster, *Nat. Rev. Drug Discovery*, 2021, **20**(8), 583.
14 J. Tong, P. Harris, M. Brimble and I. Kavianinia, *Molecules*, 2021, **26**(19), 5847.
15 U.S. National Library of Medicine, **https://clinicaltrials.gov/**, **https://beta.clinicaltrials.gov/study/NCT01954992**, accessed February 2024.
16 K. Miura, M. Kinouchi, K. Ishida, W. Fujibuchi, T. Naitoh, H. Ogawa, T. Ando, N. Yazaki, K. Watanabe, S. Haneda, C. Shibata and I. Sasaki, *Cancers*, 2010, **2**(3), 1717.
17 N. Ahmad, A. Albassam, M. Khan, Z. Ullah, T. Buheazah T, H. AlHomoud and H. Al-Nasif, *Saudi J. Biol. Sci.*, 2022, **29**(5), 3704.
18 Meta-analysis Group In Cancer, P. Piedbois, P. Rougier, M. Buyse, J. Pignon, L. Ryan, R. Hansen, B. Zee, B. Weinerman, J. Pater, C. Leichman, J. Macdonald, J. Benedetti, J. Lokich, J. Fryer, G. Brufman, R. Isacson, A. Laplanche and E. Levy, *J. Clin. Oncol.*, 1998, **16**(1), 301.
19 European Medicines Agency, Xeloda (Capecitabine), **https://www.ema.europa.eu/en/medicines/human/EPAR/xeloda**, accessed February 2024.
20 P. García-Alfonso, A. Muñoz Martín, L. Ortega Morán, J. Soto Alsar, G. Torres Pérez-Solero, M. Blanco Codesido, P. Calvo Ferrandiz and S. Grasso Cicala, *Ther. Adv. Med. Oncol.*, 2021, **13**, 1.
21 X. Jia, X. Liu, J. Wang, M. Wang, H. Guo and M. Liu, *Chem. Res. Chin. Univ.*, 2015, **31**, 78.
22 V. Jhansi Rani, A. Raghavendra, P. Kishore, Y. Nanda Kumar, K. Hema Kumar and K. Jagadeeswarareddy, *Eur. J. Med. Chem.*, 2012, **54**, 690.
23 M. Li, L. Wang, Y. Wei, W. Wang, Z. Liu, A. Zuo, W. Liu, J. Tian and H. Wang, *Pharmaceuticals*, 2022, **16**(1), 53.
24 M. Ait-Tihyaty, Z. Rachid, A. Larroque-Lombard and B. Jean-Claude, *Invest. New Drugs*, 2013, **31**(6), 1409.
25 *National Cancer Institute at the National Institutes of Health*, **https://www.cancer.gov/about-cancer/treatment/drugs/pancreatic#2**, accessed February 2024.
26 A. Lambert, C. Gavoille and T. Conroy, *Ther. Adv. Gastroenterol.*, 2017, **10**(8), 631.
27 F. Bray, J. Ferlay, I. Soerjomataram, R. Siegel, L. Torre and A. Jemal, *Ca-Cancer J. Clin.*, 2018, **68**(6), 394.
28 J. Ferlay, M. Colombet, I. Soerjomataram, T. Dyba, G. Randi, M. Bettio, A. Gavin, O. Visser and F. Bray, *Eur. J. Cancer*, 2018, **103**, 356.
29 M. Zaremba-Czogalla, A. Jaromin, K. Sidoryk, A. Zagórska, M. Cybulski and J. Gubernator, *Materials*, 2020, **13**(24), 5813.
30 L. Rocha, M. Monteiro and A. Teodoro, *Cancer Clin. Oncol.*, 2012, **1**(2), 109.

Open Access Article. Published on 23 April 2024. Downloaded on 12/9/2025 12:17:06 AM. This article is licensed under a Creative Commons Attribution-NonCommercial 3.0 Unported Licence.

31 M. Yamaguchi, T. Murata, B. El-Rayes and M. Shoji, *Oncol. Rep.*, 2015, **34**(6), 3304.
32 K. Espíndola, R. Ferreira, L. Narvaez, A. Silva Rosario, A. da Silva, A. Silva, A. Vieira and M. Monteiro, *Front. Oncol.*, 2019, **9**, 541.
33 X. Zhang, X. He, Q. Chen, J. Lu, S. Rapposelli and R. Pi, *Bioorg. Med. Chem.*, 2018, **26**(3), 543.
34 S. Khargharia, R. Rohman and R. Kar, *ChemistrySelect*, 2022, **7**(24), e202201440.
35 M. Cybulski, K. Sidoryk, M. Zaremba-Czogalla, B. Trzaskowski, M. Kubiszewski, J. Tobiasz, A. Jaromin and O. Michalak, *Int. J. Mol. Sci.*, 2024, **25**(5), 2573.
36 A. Trachtenberg, S. Muduli, K. Sidoryk, M. Cybulski and M. Danilenko, *Front. Pharmacol*, 2019, **10**, 507.
37 J. Ciccolini, C. Mercier and G. Milano, Genomics and Pharmacogenomics in Anticancer Drug Development and Clinical Response, *Cancer Drug Discovery and Development™*, ed. F. Innocenti, Humana Press, 2008, DOI: 10.1007/978-1-60327-088-5_14.
38 D. Wang, L. Zou, Q. Jin, J. Hou, G. Ge and L. Yang, *Acta Pharm. Sin. B*, 2018, **8**(5), 699.
39 L. Di, *Curr. Drug Metab.*, 2019, **20**(2), 91.
40 M. Capello, J. Fahrmann, M. Rios Perez, J. Vykoukal, E. Irajizad, S. Tripathi, D. Roife, L. Bantis, Y. Kang, D. Kundnani, H. Xu, L. Prakash, J. Long, H. Katayama, A. Fleury, S. Ferri-Borgogno, D. Baluya, J. Dennison, C. Aguilar-Bonavides, J. Casabar, M. Celiktas, K. Do, O. Fiehn, A. Maitra, H. Wang, Z. Feng, P. Chiao, M. Katz, J. Fleming and S. Hanash, *JCO Precis. Oncol.*, 2020, **4**, 426.
41 M. Capello, M. Lee, H. Wang, I. Babel, M. Katz, J. Fleming, A. Maitra, H. Wang, W. Tian, A. Taguchi, S. Hanash and J. Natl, *Cancer. Inst.*, 2015, **107**(8), djv132.
42 Y. Chen, M. Capello, M. Rios Perez, J. Vykoukal, D. Roife, Y. Kang, L. Prakash, H. Katayama, E. Irajizad, A. Fleury, S. Ferri-Borgogno, D. Baluya, J. Dennison, K. Do, O. Fiehn, A. Maitra, H. Wang, P. Chiao, M. Katz, J. Fleming, S. Hanash and J. Fahrmann, *Mol. Metab.*, 2022, **56**, 101426.
43 Global Burden of Disease 2019 Cancer Collaboration, *JAMA Oncol.*, 2022, **8**(3), 420.
44 K. Chun and S. Joo, *Biomol. Ther.*, 2022, **30**(6), 479.
45 M. Friedman and H. Jürgens, *J. Agric. Food Chem.*, 2000, **48**(6), 2101.
46 P. G. M. Wuts, *Greene's Protective Groups in Organic Synthesis*, Wiley, edn 5, 2014.
47 R. Crouch, *Tetrahedron*, 2004, **60**, 5833.
48 D. Rabiej-Kozioł, M. Krzemiński and A. Szydłowska-Czerniak, *Materials*, 2020, **13**, 4536.
49 A. Franks, Q. Wang and K. Franz, *Bioorg. Med. Chem. Lett.*, 2015, **25**(21), 4843.
50 L. Bian, S. Cao, L. Cheng, A. Nakazaki, T. Nishikawa and J. Qi, *ChemMedChem*, 2018, **13**, 1972.
51 J. Giessel, A. Loesche, R. Csuk and I. Serbian, *Eur. J. Med. Chem.*, 2019, **177**, 259.
52 M. D'Ambrosio, *Food Chem.*, 2013, **138**(4), 2079.
53 L. Monteiro, S. Oliveira, F. Paiva-Martins, P. Ferreira, D. Pereira, P. Andrade and P. Valentão, *Tetrahedron*, 2017, **73**(43), 6199.
54 M. Spasova, V. Kortenska-Kancheva, I. Totseva, G. Ivanova, L. Georgiev and T. Milkova, *J. Pept. Sci.*, 2006, **12**(5), 369.
55 K. Takao, K. Toda, T. Saito and Y. Sugita, *Chem. Pharm. Bull.*, 2017, **65**(11), 1020.
56 P. Rajan, I. Vedernikova, P. Cos, D. Berghe, K. Augustyns and A. Haemers, *Bioorg. Med. Chem. Lett.*, 2001, **11**(2), 215.
57 G. Quéléver, S. Burlet, C. Garino, N. Pietrancosta, Y. Laras and J. Kraus, *J. Comb. Chem.*, 2004, **6**(5), 695.
58 S. Gaikwad, M. Gaikwad and P. Lokhande, *J. Heterocyclic Chem.*, 2021, **58**, 1408.
59 P. Lokhande and B. Nawghare, *Indian J. Chem., Sect. B: Org. Chem. Incl. Med. Chem.*, 2012, **51**(1), 328.
60 M. Nagaraju, A. Krishnaiah and H. Mereyala, *Synth. Commun.*, 2007, **37**(15), 2467.
61 N. Shimma, I. Umeda, M. Arasaki, C. Murasaki, K. Masubuchi, Y. Kohchi, M. Miwa, M. Ura, N. Sawada, H. Tahara, I. Kuruma, I. Horii and H. Ishitsuka, *Bioorg. Med. Chem.*, 2000, **8**(7), 1697.
62 T. Mosmann, *J. Immunol. Methods*, 1983, **65**, 55.
63 B. Liu, L. Ezeogu, L. Zellmer, B. Yu, N. Xu and D. Liao, *Cancer Med.*, 2015, **4**(9), 1394.
64 C. Lipinski, F. Lombardo, B. Dominy and P. Feeney, *Adv. Drug Delivery Rev.*, 2001, **46**(1–3), 3.
65 B. Doak, B. Over, F. Giordanetto and J. Kihlberg, *Chem. Biol.*, 2014, **21**(9), 1115.
66 M. Sanguinetti and M. Tristani-Firouzi, *Nature*, 2006, **440**(7083), 463.
67 P. Banerjee, A. Eckert and A. Schrey, *Nucleic Acids Res.*, 2018, **46**(W1), W257.
68 S. Mousavi and M. Fatemi, *Bioorg. Chem.*, 2019, **90**, 103037.
69 J. Ghuman, P. Zunszain, I. Petitpas, A. Bhattacharya, M. Otagiri and S. Curry, *J. Mol. Biol.*, 2005, **353**(1), 38.
70 N. Bukowski, J. Pandey, L. Doyle, T. Richard, C. Anderson and Y. Zhu, *Bioconjug. Chem.*, 2014, **25**(12), 2189.
71 N. Filipczak, A. Jaromin, A. Piwoni, M. Mahmud, C. Sarisozen, V. Torchilin and J. Gubernator, *Cancers*, 2019, **11**(12), 1982.
72 M. Fandzloch, A. Jaromin, M. Zaremba-Czogalla, A. Wojtczak, A. Lewińska, J. Sitkowski, J. Wiśniewska, I. Łakomska and J. Gubernator, *Dalton Trans.*, 2020, **49**(4), 1207.
73 A. Jaromin, S. Parapini, N. Basilico, M. Zaremba-Czogalla, A. Lewińska, A. Zagórska, M. Walczak, B. Tyliszczak, A. Grzeszczak, M. Łukaszewicz, Ł. Kaczmarek and J. Gubernator, *Bioact. Mater.*, 2020, **6**(4), 1163.
74 O. Michalak, M. Cybulski, W. Szymanowski, A. Gornowicz, M. Kubiszewski, K. Ostrowska, P. Krzeczyński, K. Bielawski, B. Trzaskowski and A. Bielawska, *Int. J. Mol. Sci.*, 2023, **24**(10), 8875.
75 P. Krzeczyński, M. Dutkiewicz, O. Zegrocka-Stendel, B. Trzaskowski and K. Koziak, *Molecules*, 2023, **28**(5), 2287.
76 K. Ostrowska, A. Leśniak, W. Gryczka, Ł. Dobrzycki, M. Bujalska-Zadrożny and B. Trzaskowski, *Int. J. Mol. Sci.*, 2023, **24**(3), 2779.
77 S. Kim, J. Chen, T. Cheng, A. Gindulyte, J. He, S. He, Q. Li, B. Shoemaker, P. Thiessen, B. Yu, L. Zaslavsky, J. Zhang and E. Bolton, *Nucleic Acids Res.*, 2023, **51**(D1), D1373.

© 2024 The Author(s). Published by the Royal Society of Chemistry

Open Access Article. Published on 23 April 2024. Downloaded on 12/9/2025 12:17:06 AM.
This article is licensed under a Creative Commons Attribution-NonCommercial 3.0 Unported Licence.

78 O. Trott and A. Olson, *J. Comput. Chem.*, 2010, **31**(2), 455.
79 J. Jumper, R. Evans, A. Pritzel, T. Green, M. Figurnov, O. Ronneberger, K. Tunyasuvunakool, R. Bates, A. Žídek, A. Potapenko, A. Bridgland, C. Meyer, S. Kohl, A. Ballard, A. Cowie, B. Romera-Paredes, S. Nikolov, R. Jain, J. Adler, T. Back, S. Petersen, D. Reiman, E. Clancy, M. Zielinski, M. Steinegger, M. Pacholska, T. Berghammer, S. Bodenstein, D. Silver, O. Vinyals, A. Senior, K. Kavukcuoglu, P. Kohli and D. Hassabis, *Nature*, 2021, **596**(7873), 583.
80 G. Morris, R. Huey, W. Lindstrom, M. Sanner, R. Belew, D. Goodsell and A. Olson, *J. Comput. Chem.*, 2009, **30**(16), 2785.